Supporting Information Appendix for

Elevated levels of diesel range organic compounds in groundwater near Marcellus gas operations are derived from surface activities

Brian D. Drollette[a], Kathrin Hoelzer[b], Nathaniel R. Warner[c], Thomas H. Darrah[d], Osman Karatum[e], Megan P. O'Connor[e], Robert K. Nelson[f], Loretta A. Fernandez[g], Christopher M. Reddy[f] Avner Vengosh[h], Robert B. Jackson[i], Martin Elsner[b], Desiree L. Plata[a]

[a] Department of Chemical and Environmental Engineering, Yale University, New Haven, CT 06511
[b] Institute of Groundwater Ecology, Helmholtz Zentrum München, Germany
[c] Department of Civil and Environmental Engineering, Pennsylvania State University, University Park, PA 16802
[d] School of Earth Sciences, The Ohio State University, Columbus, OH 43210
[e]Department of Civil and Environmental Engineering, Duke University, Durham, NC 27708
[f] Department of Marine Chemistry and Geochemistry, Woods Hole Oceanographic Institution, Woods Hole, MA 02543
[g] Departments of Civil and Environmental Engineering and Marine and Environmental Sciences, Northeastern University, Boston, MA 02115
[h] Division of Earth and Ocean Sciences, Duke University, Durham, NC 27708
[i] School of Earth, Energy, and Environmental Sciences, Woods Institute for the Environment, and Precourt Institute for Energy, Stanford University, Stanford, CA 94305

Corresponding Author: Desiree L. Plata; desiree.plata@yale.edu

Keywords: hydrophobic organic compounds, groundwater, high volume hydraulic fracturing, natural gas extraction

Analytical Methods

Sample Collection: Groundwater wells were purged until temperature, pH, and electrical conductance readings were stable. Shallow groundwater samples were collected in pre-combusted 40-mL glass volatile organic analysis (VOA) vials containing 1-mL of 50% v/v hydrochloric acid (HCl), capped without headspace, and stored on ice or at 4^{o}C until analysis. Samples were collected as close to the wellhead as possible and upstream of any water treatment systems.

Volatile Organic Compounds (VOCs): We used a modified version of EPA Method 624 and 8015D as described in Getzinger et al. (2015) [1] for quantification and qualitative identification of 50 unique VOCs via GC-FID and GC-MS (Table S1). Briefly, a 5-mL aliquot of groundwater was purged with helium on a purge and trap concentrator and subsequently transferred to a GC-FID (quantification with retention time identity confirmation) or GC-MS (confirming qualitative identification) using a Restek MegaMix^{TM} standard mixture (Restek 502.2).

Gasoline Range Organic Compounds (GRO): We quantified GRO with the sample preparation techniques described for the VOC analysis and used a GRO mix standard for quantification (Restek #30065), following EPA Method 8015D. Chromatographic peaks eluting within the retention time window of 2-methylpentane and 1,2,4-trimethylbenzene were integrated and added together for a total signal representative of the organic compounds with boiling points within the defined gasoline range [2].

Diesel Range Organic Compounds (DRO): We used a liquid-liquid extraction technique to quantify DRO with EPA Method 8015D, as described in Getzinger et al. (2015) [1]. Approximately 500 mL of groundwater was extracted with 90:10 dichloromethane:methanol three times before rotary evaporation down to a final volume of 1-1.5 mL. Samples were quantified with a Restek DRO mix standard (Restek 31064) via GC-FID. Chromatographic peaks eluting within the retention time window of decane ($_{n}C_{10}$) and octacosane ($_{n}C_{28}$) were integrated and added together for a total signal representative of the organic compounds with boiling points within the defined diesel range [2].

Comprehensive two-dimensional gas chromatography: Two Leco GC×GC systems were used in this study: one coupled with a time-of-flight mass spectrometer (TOF-MS; Leco Pegasus 4D) and one coupled to a flame ionization detector (FID) detector. They were equipped with an Agilent 6890 GC (TOF-MS) and Agilent 7890 GC (FID system) and configured with split/splitless auto injectors (7683B series) and a dual stage cryogenic modulator (Leco, Saint Joseph, Michigan). Samples were injected in splitless mode. Two capillary GC columns were fitted in each GC×GC instrument, with a cryogenic modulator between the two. The first-dimension column was a non-polar Restek Rxi-1ms, (60 m length, 0.25 mm I.D., 0.25 μm film thickness) and the second-dimension separations were performed on a 50% phenyl polysilphenylene-siloxane column (SGE BPX50, 1.0 m length, 0.10 mm I.D., 0.1 μm film thickness). The modulator between the two columns operates with a liquid N_2 cold jet and dry N_2 hot jet operated at 10-15 °C above the temperature of the main GC oven. Hydrogen was used as carrier gas at a

constant flow rate of 0.90 mL min^{-1} on the GC×GC-FID and helium at a flow rate of 1.00 mL min^{-1} on the GC×GC-TOF.

GC×GC-TOFMS Method:
The temperature program of the main oven started isothermal at 50 °C (15 min) and was then ramped from 50 to 330 °C at 1.75 °C min^{-1}. The hot jet pulse width was 0.75 s and the modulation period was 10 s with a 4.25 s cooling period between stages. The second dimension oven was programmed from 55 °C (15 min) to 335 °C at 1.75 °C min^{-1}. The TOF-MS data were sampled at an acquisition rate of 50 spectra per second. The transfer line from the second oven to the TOFMS was deactivated fused silica (0.5 m length, 0.18 mm I.D.), constantly held at 315 °C. The TOF detector voltage was 1335 Volts and the source temperature 220 °C. The mass spectrometer employs 70 eV electron ionization and operates at a push pulse rate of 5 kHz allowing sufficient signal averaging time to ensure good signal-to-noise ratios while still operating at a high enough data acquisition rate to accurately process (signal average) spectra from the peaks eluting from the second dimension column in this high resolution separation technique (GC×GC-TOF second dimension peak widths range between 50 to 200 milliseconds).

GC×GC-FID Method:
For the GC×GC-FID analysis, 1 µL of each sample solution was injected into a 300 °C splitless injector with a purge time of 0.5 min. The first-dimension column and the dual stage cryogenic modulator resided in the main oven, whereas the second-dimension column was fitted in a separate oven, allowing for independent temperature control of all three. The temperature program of the main oven started isothermal at 40 °C (10 min) and was then ramped from 40 to 335 °C at 1.25 °C min^{-1}. The second dimension oven was programmed to remain isothermal at 45 °C for 10 minutes and then ramped from 45 to 340 °C at 1.25 °C min^{-1}. The hot jet pulse width was 0.50 seconds and the modulation period was 7.5 seconds with a 3.25 second cooling period between stages.

Inorganic constituents: Inorganic compounds were analyzed from samples collected either simultaneously with or prior to sample collection campaigns for organic compounds. Analyses were performed via methods described by Warner et al. (2012) [3].

Methane: Methane was analyzed from samples collected simultaneously with or prior to sample collection campaigns for organic compounds. Analyses were performed via methods described by Jackson et al. (2013) and Darrah et al. (2014) [4, 5].

Helium concentrations and noble gases: Helium and heavier noble gases were analyzed from samples collected simultaneously with or prior to sample collection campaigns for organic compounds. Analyses were performed via methods described by Jackson et al. (2013) and Darrah et al. (2014) [4, 5].

Field Setting
Samples were collected in northeastern Pennsylvania from three aquifers (Lock Haven, Catskill, and Alluvium) overlying the Marcellus Shale in the northern Appalachian Basin. Extensive descriptions of the geology and hydrogeologic settings can be found elsewhere [3-7].

Groundwater Contaminant Transport Calculations

Subsurface groundwater transport of bis(2-ethylhexyl) phthalate through an aquifer representative of northeastern Pennsylvania hydrogeology was estimated based on calculations and physical parameters (Table S2) from various sources [8-13].

The compound-specific, sorption-retarded transport velocity, v_c, is given by:

$$v_c = \frac{v_w}{R} \qquad \textit{Eq. S1}$$

where v_w is the bulk groundwater flow and R is the retardation factor given by:

$$R = 1 + \rho_s \frac{1-\phi}{\phi} K_d \qquad \textit{Eq. S2}$$

and ρ_s is the sediment or soil bulk density, ϕ is the porosity, and K_d is the solid-water distribution coefficient. Here, we assume K_d is dominated by sorption to non-black carbon organic carbon phases [10], and so:

$$K_d = K_{oc} * f_{oc} \qquad \textit{Eq. S3}$$

where K_{oc} is the organic carbon partition coefficient and f_{oc} is the fraction of organic carbon in the porous medium.

Modeling chemical transport across a polyethylene liner

We deployed an analytical solution to calculate 1-D Fickian diffusion of bis(2-ethylhexyl) phthalate (DEHP; diethylhexyl phthalate) across a 4-mm polyethylene (PE) film, following Crank (1975) [14] and Schwarzenbach et al. (2002) [10]:

$$C_{PE}(x,t) = C_{PE}^{*} erfc\left(\frac{x}{2(D_{PE}t)^{1/2}}\right) \qquad \textit{Eq. S4}$$

where $C_{PE}(x,t)$ (mass/cm^3) is the concentration in the PE x cm from the side in contact with retention pond water at some time, t (s), C_{PE}^{*} is the concentration at the boundary of the PE equilibrated with water in the retention pond, and D_{PE} (cm^2/s) is the diffusivity of DEHP within the PE. By neglecting the additional resistances to mass transport provided by a water-side diffusive boundary layer, diffusion within the soil porous media, and retardation within the PE caused by pigments (e.g., carbon black, commonly used to color the black PE liners used in containment ponds), this mathematical model simulates the furthest possible distance the concentrations front could reach within the PE film. D_{PE} for DEHP was estimated at $10^{-11.3}$ cm^2/s, based on a relationship between molar volume (MV) and log D_{PE} (Eq. S5) obtained from measured D_{PE} for PAHs (polycyclic aromatic hydrocarbons) and PCBs (polychlorinated biphenyls) [15] and molar volume

estimated using the Sparc Performs Automated Reasoning in Chemistry (SPARC) chemical property estimator.

$$\log D_{PE}\ (cm^2/s) = -0.014\ MV\ (cm^3/mol) - 6.1 \qquad Eq.\ S5$$

Using these values, DEHP will only diffuse 1 mm into the PE liner after 4 years (and only 2 x 10^{-27} % of the original concentration). Using an even more conservative calculation, employing 100-fold faster diffusion ($D_{PE}=10^{-9.3}$ cm^2/s) indicates that only 2% of DEHP could cross a 4-mm thick PE liner by 12 months.

We confirmed the application of the analytical solution by running an explicit, finite-difference model to simulate transport across the PE using a previously prepared Matlab code modified to reflect boundary conditions relevant to a pond-PE-porous media system [16].

Table S1. Detection limits for DRO, GRO, and the targeted VOCs.

Compound	*LOD (ppb)*	*Compound*	*LOD (ppb)*
DRO	0.09	1,2-Dibromoethane	0.17
GRO	0.03	chlorobenzene	1.8
1,1-Dichloroethene	0.84	Ethylbenzene	2.9
Methylene chloride	1.0	m-Xylene+p-xylene	5.0
1,1-Dichloroethane	0.47	o-xylene	2.4
trans-1,2-Dichloroethene	1.2	styrene	0.26
2,2-Dichloropropane	2.4	bromoform	9.0
cis-1,2-dichloroethene	2.4	1,2,3-Trichloropropane	0.32
chloroform	2.7	Bromobenzene	0.54
Bromochloromethane	1.5	1,1,2,2-Tetrachloroethane	1.2
carbon tetrachloride	0.83	n-Propylbnezene	0.34
1,1,1-trichloroethane	0.83	2-Chlorotoluene	0.39
1,1-dichloropropene	0.83	1,3,5-Trimethylbenzene	0.19
Benzene	0.20	tert-Butylbenzene	0.37
1,2-dichloroethane	0.53	1,2,4-Trimethylbenzene	0.35
Trichloroethene	1.2	sec-Butylbenzene	0.42
1,2-Dichloropropane	0.70	1,3-Dichlorobenzene	0.55
bromodichloromethane	4.2	1,4-Dichlorobenzene	0.24
Dibromomethane	4.1	4-isopropyltoluene	0.24
cis-1,3-Dichloropropene	0.91	1,2-Dichlorobenzene	0.56
toluene	0.26	n-Butylbenzene	0.50
trans-1,3-Dichloropropene	1.2	1,2-Dibromo-3-chloropropane	7.2
1,1,2-Trichloroethane	1.5	1,2,4-Trichlorobenzene	1.0
Tetrachloroethene	0.41	Hexachlorobuatdiene	2.6
1,3-Dichloropropane	0.66	Napthalene	0.88
dibromochloromethane	0.10	1,2,3-Trichlorobenzene	1.1

167
168

Table S2. Parameters used for subsurface transport calculations of bis(2-ethylhexyl) phthalate.

Variable	High velocity	Low velocity
$K_{oc\ \text{bis(2-ethylhexyl) phthalate}}$	4.998	5.078
f_{oc} ($kg_{oc}\ kg_{sed}^{-1}$)	0.001	0.1
ρ_s ($kg\ L^{-1}$)	1.6	2.4
ϕ	0.08	0.25
v_w ($km\ yr^{-1}$)	8.219	0.109
v_c ($km\ yr^{-1}$)	7.527	0.0234

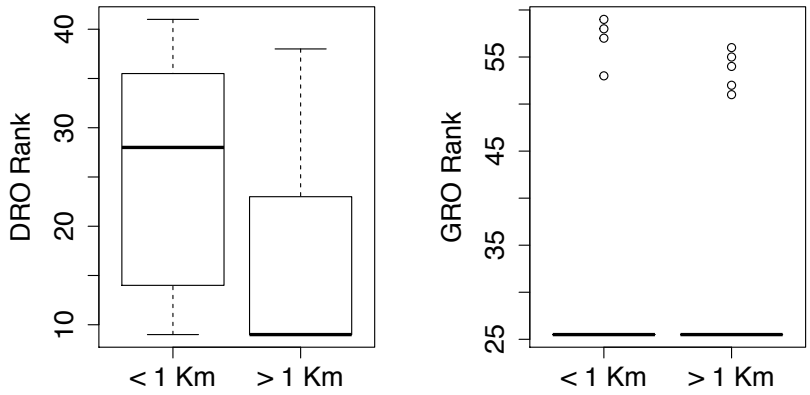

Figure S1. Ranked comparison of DRO (left) and GRO (right) between active and non-active zones (active zone defined as < 1 km from a shale gas well). There was a statistical difference in DRO between zones (p = 0.01, Mann-Whitney U test) and no difference in GRO between zones (p = 0.90).

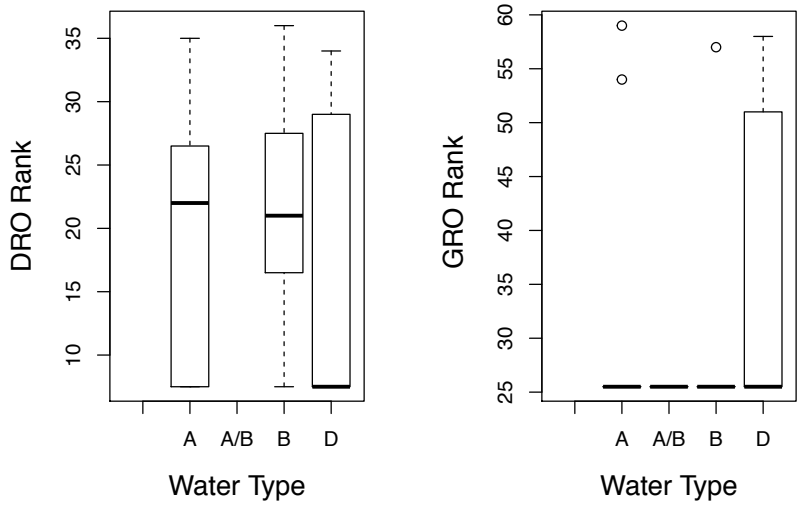

Figure S2. Ranked comparison of DRO (left) and GRO (right) with respect to different shallow groundwater types. Type D water has influence of Marcellus formation brine via natural connectivity [3]. There were no statistical differences in DRO or GRO between types (DRO, $p > 0.05$; GRO, $p > 0.05$; Kruskal-Wallis test).

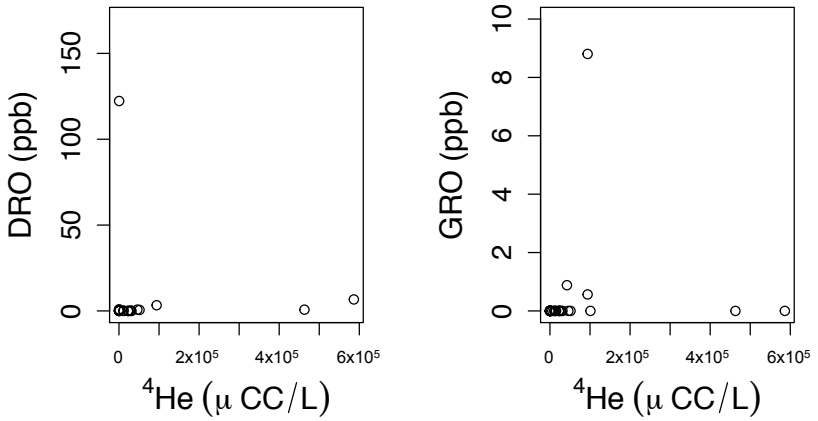

Figure S3. Relationship of DRO (left) and GRO (right) with respect to ^{4}He measurements taken either during the same sampling campaign or at a previous time. Statistical analysis showed no correlation (DRO, $p > 0.05$; GRO, $p > 0.05$, Spearman correlation).

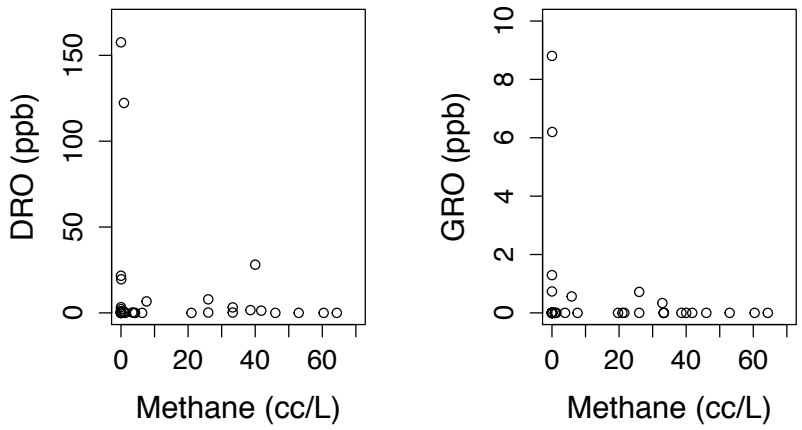

Figure S4. Relationship of DRO (left) and GRO (right) concentrations with respect to methane measurements taken either during the same sampling campaign or at a previous time. Statistical analyses showed no correlation (DRO, $p > 0.05$; GRO $p > 0.05$, Spearman correlation).

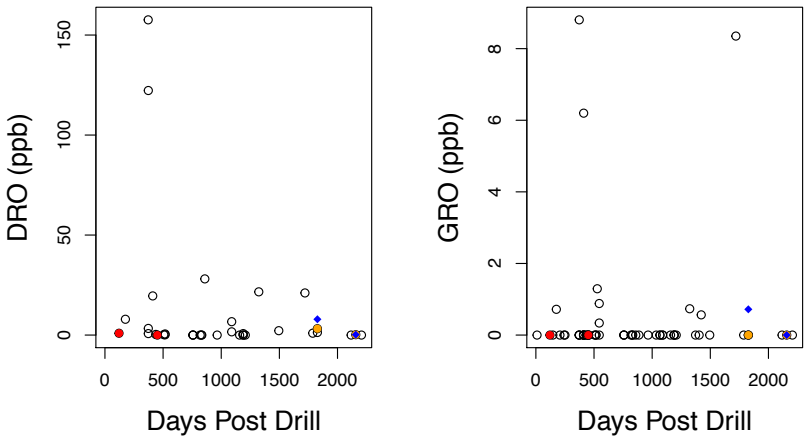

Figure S5. Relationship of DRO (left) and GRO (right) with the number of days since the nearest shale gas well was drilled. Statistical analyses showed no correlation (DRO, $p > 0.05$; GRO, $p > 0.05$, Spearman correlation). Note that only three groundwater wells were sampled repeatedly over a period of time (shown in color), and most of the data are individual wells that were sampled once during our three-year period.

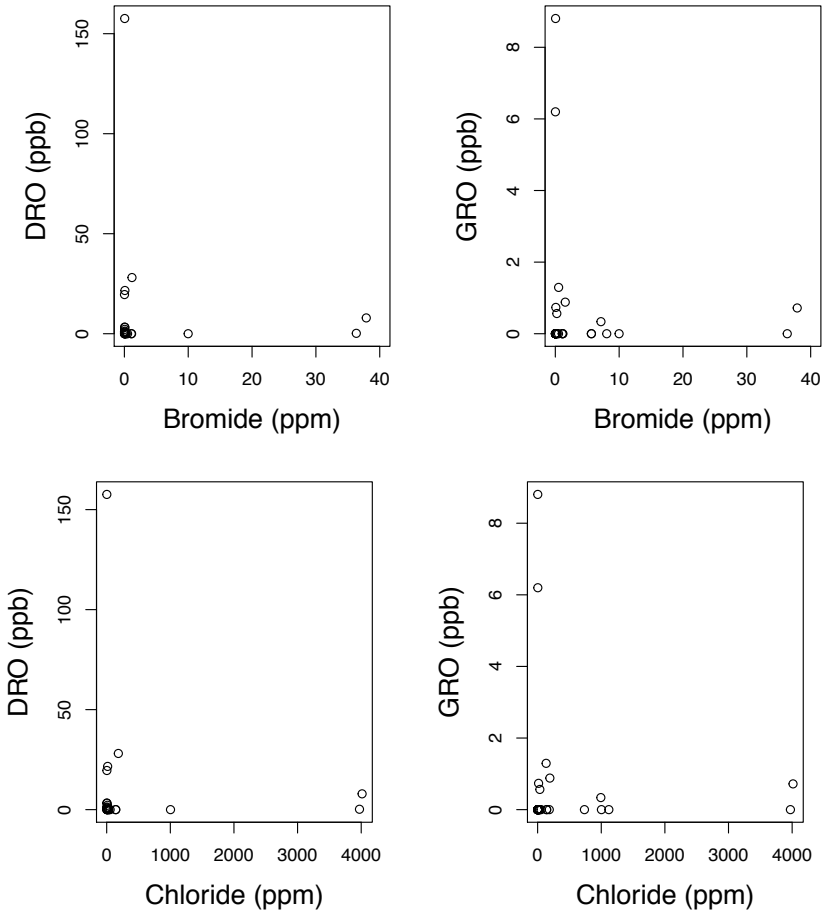

Figure S6. Relationship of DRO (left) and GRO (right) with bromide (top) and chloride (bottom). Statistical analyses showed no correlation (DRO and bromide, $p > 0.05$; GRO and bromide, $p > 0.05$; DRO and chloride, $p > 0.05$; GRO and chloride, $p > 0.05$).

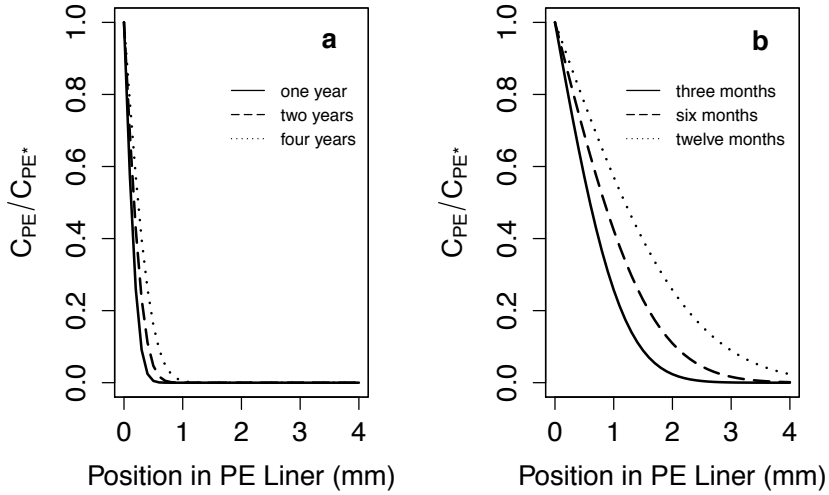

Figure S7. The 1-dimensional Fickian diffusion model for transport of bis(2-ethylhexyl)phthalate through a 4-mm thick polyethylene liner using a reasonable, estimated diffusivity of $10^{-11.3}$ cm^2/s (a) and a 100-fold faster diffusion of $10^{-9.3}$ cm^2/s (b). Note that this model represents the fastest-possible transport times, as we neglected resistances to mass transport provided by a water-side diffusive boundary layer, diffusion within the soil porous media, and retardation within the PE caused by pigments (e.g., carbon black, commonly used to color the black PE liners used in containment ponds).

GRO and DRO Fingerprinting

GRO/DRO ratios could be used as a tracer of these waters or potentially as an indicator of deep formation water migration. Noting that only a small number of samples (n = 5) had detectable levels of both GRO *and* DRO, it is clear that there is no discernable GRO/DRO "fingerprint" (Figure 2, inset, main text) in groundwater in from this region. Similarly, flowback water showed variable GRO/DRO ratios, with total GRO and DRO abundance much higher than that observed in groundwater (SI Fig. S8). Thus, GRO/DRO fingerprinting and enrichments are not viable candidates for tracing flowback water migration from either faulty well casings or leaking containment pits.

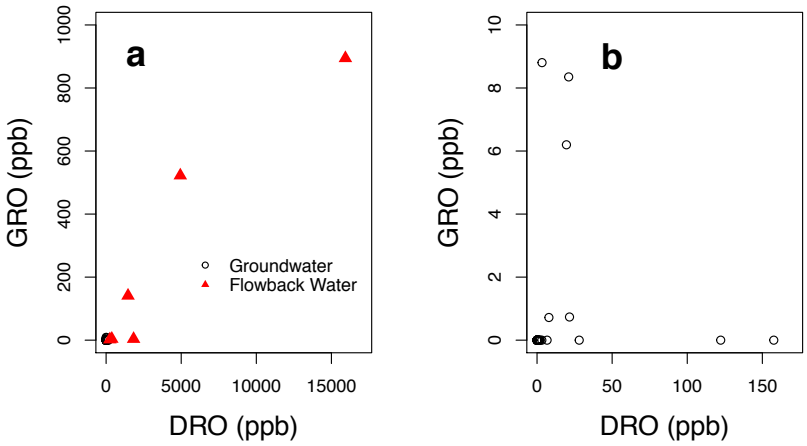

Figure S8. Comparison of GRO and DRO concentrations in shallow groundwater samples and flowback waters samples. Note that the flowback water samples (colored triangles) have much higher GRO and DRO (a), whereas groundwater samples (open circles) have comparatively low levels for GRO and DRO (b). There is no discernable GRO/DRO fingerprint in either groundwater or flowback water, as both exhibit a high degree of variability.

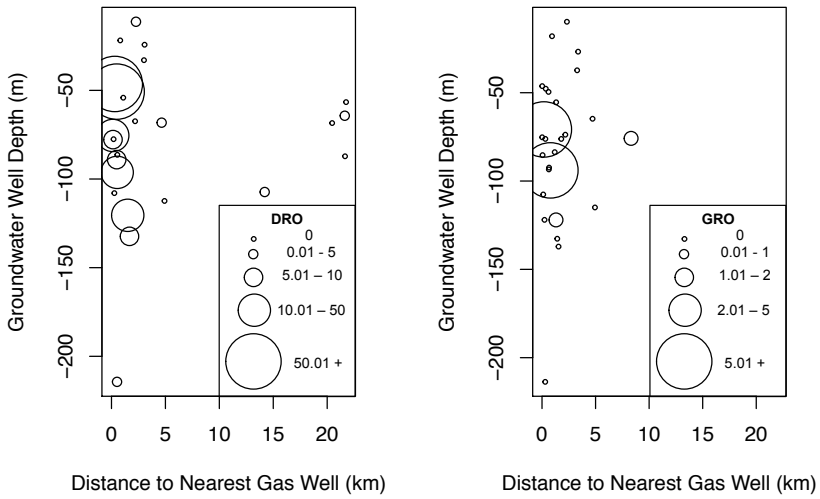

Figure S9. Relationship of DRO (left) and GRO (right) concentrations with sampled groundwater well depth and the distance to the nearest shale gas well. There was no statistical relationship between concentration and well depth (DRO $p > 0.05$, GRO $p > 0.05$). The samples with the highest concentrations were found in areas with relatively shallow well depths and close to shale gas wells.

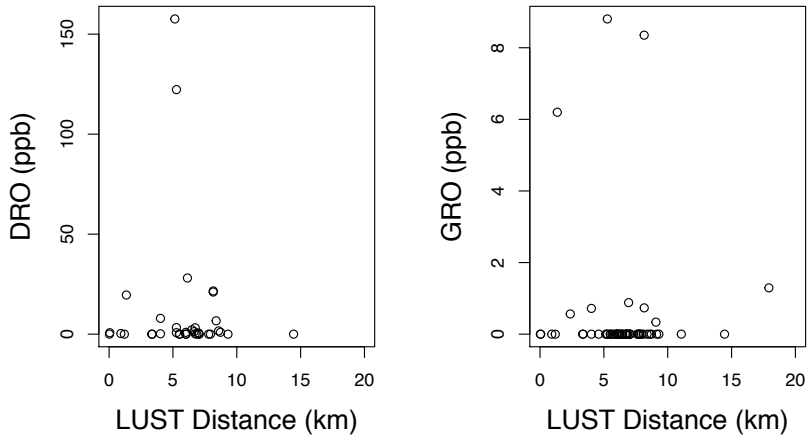

Figure S10. Spatial relationship of DRO (left) and GRO (right) concentrations with the distance to the nearest leaking underground storage tank (LUST) as reported by Pennsylvania Department of Environmental Protection (PA DEP). Statistical analyses showed no correlation (DRO, $p > 0.05$; GRO, $p > 0.05$). LUST location data available at http://www.depreportingservices.state.pa.us/ReportServer/Pages/ReportViewer.aspx?/Cleanup/Tank_Cleanup_Incidents. Accessed on November 2, 2014.

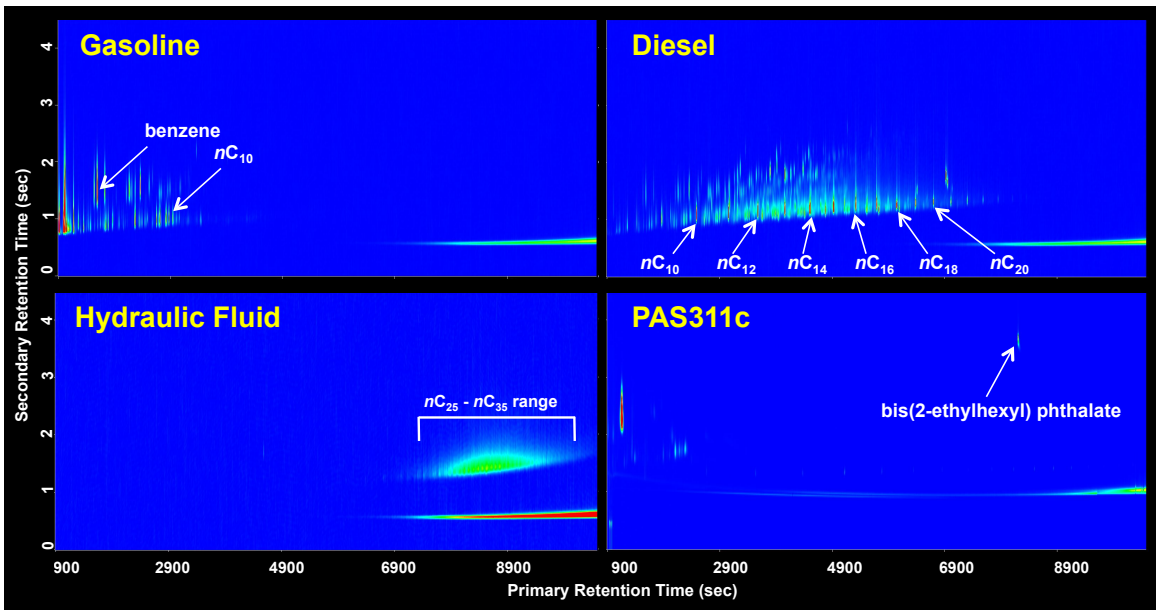

Figure S11. GCxGC-TOFMS analysis of gasoline, diesel fuel, and a hydraulic fluid common in industrial and agricultural applications, along with a groundwater samples (PAS 311C) that contained elevated levels of DRO. Note that the instrument response in the DRO region of the groundwater sample is dominated by the phthalate and unlike those of the fuels.

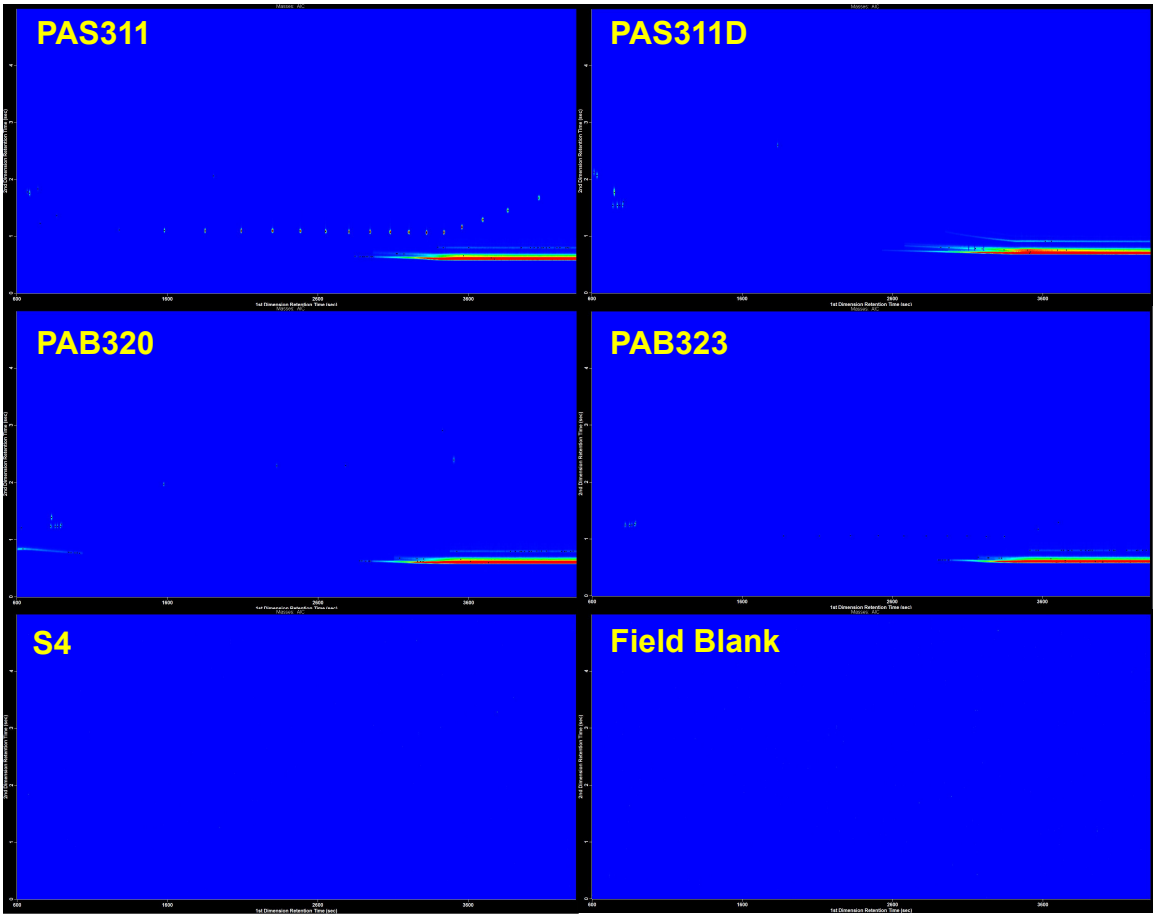

Figure S12. GCxGC-TOF-MS analysis of five (out of 23 total) low-but-detectable-DRO containting groundwater samples and a field blank indicated no detectable levels of bis(2-ethyhexyl) phthalate. These results demonstrate that phthalates, while ubiquitous in industrial products (e.g., plastics and piping material), do not often appear in groundwater in this region. The complimentary analysis of two high-DRO containing groundwater samples appears in the main text and shows the presence bis(2-ethylhexyl) phthalate.

References

1. Getzinger et al. (2015) Natural Gas Residual Fluids: Sources, Endpoints, and Organic Chemical Composition after Centralized Waste Treatment in Pennsylvania. *Environ Sci Technol* 49(14):8347-8355.

2. US Environmental Protection Agency (2003) *Method 8015D Nonhalogenated Organics Using GC/FID.* (US EPA, Washington DC).

3. Warner NR, et al. (2012) Geochemical evidence for possible natural migration of Marcellus Formation brine to shallow aquifers in Pennsylvania. *Proc Natl Acad Sci USA* 109(30):11961-11966.

4. Jackson RB, et al. (2013) Increased stray gas abundance in a subset of drinking water wells near Marcellus shale gas extraction. *Proc Natl Acad Sci USA* 110(28):11250-11255.

5. Darrah TH, Vengosh A, Jackson RB, Warner NR, & Poreda RJ (2014) Noble gases identify the mechanisms of fugitive gas contamination in drinking-water wells overlying the Marcellus and Barnett Shales. *Proc Natl Acad Sci USA* 111(39):14076-14081.

6. Faill RT (1997) A geologic history of the north-central Appalachians. 1. Orogenesis from the mesoproterozoic through the tectonic orogeny. *Am J Sci* 297(6):551-619.

7. Faill RT (1997) A geologic history of the north-central Appalachians. 2. The Appalachian basin from the Silurian through the Carboniferous. *Am J Sci* 297(7):729-761.

8. Rogers JD, Burke TL, Osborn SG, & Ryan JN (2015) A Framework for Identifying Organic Compounds of Concern in Hydraulic Fracturing Fluids Based on Their Mobility and Persistence in Groundwater. *Environ Sci Technol Letters* 2(6): 158-164.

9. Gelhar LW, Welty C, & Rehfeldt KR (1992) A Critical Review of Data on Field-Scale Dispersion in Aquifers. *Water Resour Res* 28(7):1955-1974.

10. Schwarzenbach RP, Gschwend PM, & Imboden DM. *Environmental Organic Chemistry*. 2nd ed. 2003, Hoboken, NJ: John Wiley & Sons, Inc.

11. Todd DK & Mays LW. *Groundwater Hydrology*. 3rd ed. 2005, Hoboken, NJ: John Wiley & Sons, Inc.

12. Agency for Toxic Substances and Disease Registry (ATSDR). *Toxicological Profile for Di(2-ethylhexyl)phthalate.* Public Health Service, U.S. Department of Health and Human Services, Atlanta, GA. 1993.

13. US Environmental Protection Agency (2015). Estimation Programs Interface Suite for Microsoft® Windows, v 4.11. (US EPA, Washington DC).

14. Crank J. *The Mathematics of Diffusion*. 2nd ed. 1975, Bristol, England: Clarendon Press.

15. Rusina TP, Smedes F, Klanova J, Booij K, & Holoubek I. (2007) Polymer selection for passive sampling: A comparison of critical properties. *Chemosphere* 68(7):1344-1351.

16. Fernandez LA, MacFarlane JK, Tcaciuc AP, & Gschwend PM (2009) Measurement of Freely Dissolved PAH Concentrations in Sediment Beds Using Passive Sampling with Low-Density Polyethylene Strips. *Environ Sci Technol* 43(5):1430-1436.